Chemical evolution during the process of proto-star formation by considering a two dimensional hydrodynamic model

Ankan Das [a,*], Liton Majumdar [a], Sandip K. Chakrabarti [a,b], Sonali Chakrabarti [a,c]

[a] Indian Centre for Space Physics, 43 Chalantika, Garia Station Road, Kolkata 700084, India
[b] S.N. Bose National Center for Basic Sciences, JD-Block, Salt Lake, Kolkata 700098, India
[c] Maharaja Manindra Chandra College, 20 Ramakanto Bose Street, Kolkata 700003, India

HIGHLIGHTS

- We carried out 2D hydrodynamical simulation for the collapsing phase of a proto-star.
- Total variation diminishing scheme (TVD) is used for this purpose.
- Numerical simulations are carried out to obtain the abundances of different interstellar molecules.
- Chemical composition are noticed to be highly sensitive to the dynamic properties.
- Chemical evolution of interstellar bio-molecules are well explained.

ARTICLE INFO

Keywords:
Astrochemistry
Star formation
ISM: molecules
ISM: abundances
ISM: evolution
Methods: numerical

ABSTRACT

Chemical composition of a molecular cloud is highly sensitive to the physical properties of the cloud. In order to obtain the chemical composition around a star forming region, we carry out a two dimensional hydrodynamical simulation of the collapsing phase of a proto-star. A total variation diminishing scheme (TVD) is used to solve the set of equations governing hydrodynamics. This hydrodynamic code is capable of mimicking evolution of the physical properties during the formation of a proto-star. We couple our reasonably large gas-grain chemical network to study the chemical evolution during the collapsing phase of a proto-star. To have a realistic estimate of the abundances of bio-molecules in the interstellar medium, we include the recently calculated rate coefficients for the formation of several interstellar bio-molecules into our gas phase network. Chemical evolution is studied in detail by keeping grain at the constant temperature throughout the simulation as well as by using the temperature variation obtained from the hydrodynamical model. By considering a large gas-grain network with the sophisticated hydrodynamic model more realistic abundances are predicted. We find that the chemical composition are highly sensitive to the dynamic behavior of the collapsing cloud, specifically on the density and temperature distribution.

1. Introduction

The rate of discovery of molecules in the interstellar medium (ISM) has been increasing in the past few years and today, over 170 confirmed molecules have been observed. After the discovery of several molecules in the condensed phase, it is now believed that the icy grains play a crucial role in enriching the ISM chemically. Recent modeling results (Hasegawa et al., 1992; Chakrabarti et al., 2006a,b; Das et al., 2008b; Das and Chakrabarti, 2011) also suggest that the gas–grain interaction needs to be appropriately modeled in order to mimic the exact chemical evolution. However, the chemical evolution of any cloud is highly sensitive to the physical properties of that cloud. It is therefore essential to study the physical properties of the cloud at any instant for appropriate modeling. It is clear that the observed molecules must be synthesized during the formation of the stars (i.e., in the proto-star phase). Prior to the star formation, the interstellar chemistry mainly followed by the gas-phase ion–molecular and neutral–neutral reactions leading to the formation of small radicals and unsaturated molecules. During the collapsing phase, when the temperature is cold enough and the density is much higher, most molecules accrete onto grains and form an icy mantle (Van Dishoeck and Blake, 1998). Recent theoretical work by Majumdar et al. (2013) showed that how the computed spectrum differs in between the gas phase

* Corresponding author. Tel.: +91 3324366003; fax: +91 3324622153.
E-mail addresses: ankan@csp.res.in (A. Das), liton@csp.res.in (L. Majumdar), chakraba@bose.res.in (S.K. Chakrabarti), sonali@csp.res.in (S. Chakrabarti).

and ice phase. As the temperature starts to increase due to the formation of stars, various species would return to the gas phase at the rate determined by their binding energies with the grain surface. As a result, the gas phase chemical composition is modified by the composition of the grain mantle. In the present context, we carry out our investigation by revising our past hydro-chemical model (Das et al., 2008a). The hydrodynamical model is improved by introducing two dimensional flow (instead of one dimensional model used by Das et al. (2008a)) by the use of a scheme based on the total variation diminishing (TVD) scheme (Harten, 1983; Ryu et al., 1993).

Our chemical model consists of gas phase chemical network as well as surface chemical network. This large gas phase network includes the network of Woodall et al. (2007). In addition, we introduce some reactions which lead to the formation of bio-molecules by following Chakrabarti and Chakrabarti (2000a,b); Majumdar et al. (2012, 2013). We assume that the gas and the grains are coupled through the accretion and thermal evaporation processes. Most updated barrier energies are used for the grain chemistry network (Allen and Robinson, 1977; Das et al., 2010; Das and Chakrabarti, 2011). Our Chemical code is designed in such a way that any variation of the physical parameters such as the density & temperature are reflected in computing instantaneous rates. The plan of the paper is the following. In the next section, the formulation of the TVD scheme is discussed in details. Different aspects of our simulation results are presented and discussed in Section 3, and finally in Section 4, we summarize our work.

2. Formulation of the TVD scheme

In the past, we carried out the hydrodynamic simulation for a spherically symmetric gas cloud (Das et al., 2008a). The code was developed to study the dynamic behavior of a spherically symmetric isothermally (T = 10 K) collapsing cloud. However, in order to study the chemical evolution more realistically, it is necessary to study the dynamic behavior in a two dimensional flow which includes rotation. In the present paper, we implement these aspects.

We solve the following hyperbolic system of conservation equations for a collapsing interstellar cloud:

$$\frac{\partial \rho}{\partial t}+\frac{\partial}{\partial x_k}(\rho u_k)=0, \tag{1}$$

$$\frac{\partial(\rho u_i)}{\partial t}+\frac{\partial}{\partial x_k}(\rho u_i u_k+p\delta_{ik})=0, \tag{2}$$

$$\frac{\partial E}{\partial t}+\frac{\partial}{\partial x_k}[(E+p)u_k]=0, \tag{3}$$

where, $E=\frac{p}{(\gamma-1)}+\frac{\rho u_k^2}{2}$ is the total energy per unit volume and the rest of the variables have their usual meanings. We use the TVD scheme to solve the above hydrodynamic equations in cylindrical coordinates (r, Φ, z). Here we denote r coordinate by x and Φ by y. Harten's TVD scheme (Harten, 1983) is an explicit, second order Eulerian finite difference scheme, which solves a hyperbolic system of the conservation equations. The key merit of this scheme is to achieve a high resolution. This scheme is relatively simple to program compared to the other high accuracy numerical schemes and require less CPU time. Here we assume there are no variations along the y (Φ) direction, so the code is actually two dimensional in nature.

For the inclusion of entropy, we introduce another conservative quantity, $S=\frac{p}{\rho^{\gamma-1}}$. Combining the energy equation (Eq. (3)) with the mass conservation equation (Eq. (1)), modified entropy equation becomes

$$\frac{\partial S}{\partial t}+\frac{\partial}{\partial x_k}(Su_k)=0. \tag{4}$$

The mass and momentum conservation equations (Eqs. (1) and (2) respectively), along with the above modified entropy equation can be written in the vector form as the following:

$$\partial_t q+\partial_x F_x+\partial_y F_y+\partial_z F_z=M, \tag{5}$$

where, M is the source vector, $F_x(q), F_y(q), F_z(q)$ are the flux functions with vector q. The Jacobian matrices, $A_x(q)=\frac{\partial F_x}{\partial q}$, $A_y(q)=\frac{\partial F_y}{\partial q}$, and $A_z(q)=\frac{\partial F_z}{\partial q}$, are formed by using the flux functions. All the vectors are denoted as follows:

$$q=\begin{pmatrix}\rho\\ \rho v_x\\ \rho v_y\\ \rho v_z\\ S\end{pmatrix},\quad F_x=\begin{pmatrix}\rho v_x\\ \rho v_x^2+S\rho^{\gamma-1}\\ \rho v_x v_y\\ \rho v_x v_z\\ S v_x\end{pmatrix},\quad F_y=\begin{pmatrix}\rho v_y\\ \rho v_x v_y\\ \rho v_y^2+S\rho^{\gamma-1}\\ \rho v_y v_z\\ S v_y\end{pmatrix},$$

$$F_z=\begin{pmatrix}\rho v_z\\ \rho v_x v_z\\ \rho v_y v_z\\ \rho v_z^2+S\rho^{\gamma-1}\\ S v_z\end{pmatrix},\quad M=\begin{pmatrix}0\\ \rho v_y^2/x\\ \rho v_x v_y/x\\ 0\\ 0\end{pmatrix}. \tag{6}$$

We calculate all the eigen values using the characteristic equation or secular equation and the values are,

$$\begin{aligned}a_1&=v_x-c,\\ a_2&=v_x,\\ a_3&=v_x,\\ a_4&=v_x,\\ a_5&=v_x+c.\end{aligned} \tag{7}$$

To find the eigenvectors of A_x with respect to the eigenvalue a_1, we have considered the following eigenvalue equation,

$$(A_x-a_1 I)R_1=0, \tag{8}$$

where, I is the Unit matrix. By solving the above, the right eigenvector corresponding to the eigenvalues are calculated. The set of left eigenvectors ([L]) are determined from the inverse of the right eigenvectors ([R]):

$$[L]=[R]^{-1}. \tag{9}$$

We use the Roe approximate Riemann solution (Roe, 1981) to get the averaged values of the physical quantities at the grid boundaries:

$$\begin{aligned}\rho_{i+\frac{1}{2}}&=\frac{\rho_i+\rho_{i+1}}{2},\\ v_{x,i+1/2}&=\frac{\sqrt{\rho_i}v_{x,i}+\sqrt{\rho_{i+1}}v_{x,i+1}}{\sqrt{\rho_i}+\sqrt{\rho_{i+1}}},\\ v_{y,i+1/2}&=\frac{\sqrt{\rho_i}v_{y,i}+\sqrt{\rho_{i+1}}v_{y,i+1}}{\sqrt{\rho_i}+\sqrt{\rho_{i+1}}},\\ v_{z,i+1/2}&=\frac{\sqrt{\rho_i}v_{z,i}+\sqrt{\rho_{i+1}}v_{z,i+1}}{\sqrt{\rho_i}+\sqrt{\rho_{i+1}}},\\ S_{i+1/2}&=\frac{\sqrt{\rho_i}S_i+\sqrt{\rho_{i+1}}S_{i+1}}{\sqrt{\rho_i}+\sqrt{\rho_{i+1}}},\end{aligned} \tag{10}$$

$c_{i+1/2} = \gamma S_{i+1/2} \rho_{i+1/2}^{\gamma-2}$.

To incorporate the self-gravity in this code, we introduce gravitational potential. The source function including the self-gravity term becomes,

$$M = \begin{pmatrix} 0 \\ \rho v_y^2/x - T_x \\ \rho v_x v_y/x \\ -T_z \\ -(T_x x + T_z z) \end{pmatrix}, \quad (11)$$

where, ϕ is the potential energy per unit mass, $T_x = \rho \frac{d\phi}{dx}$ and $T_z = \rho \frac{d\phi}{dz}$ are the components along the x and z directions respectively. $\frac{d\phi}{dx}$ and $\frac{d\phi}{dz}$ are the gravitational force components per unit mass along the x and z directions respectively. Gravitational potential energy per unit mass (ϕ), is calculated as follows;

$$\phi = \phi_s + \phi_c,$$

where, ϕ_s is the potential energy per unit mass of the cloud and ϕ_c is the potential energy per unit mass due to the central core mass ($M_c(t)$) at any time t. $M_c(t)$ is increasing with time as follows:

$$M_c(t) = M_c(t) + M_s(t), \quad (12)$$

where, $M_s(t)$ is the amount of mass dumping by the cloud at the instant t. This amount depends on the physical properties of the grid from where they are contributing to the core. In our code, we assume that any mass going inside the threshold radius (R_c) at any instant t will be treated as $M_s(t)$.

2.1. Effects of heating and cooling

There are various physical processes which could affect the physical properties of the ISM, such as, heating and cooling of the interstellar medium. Molecular clouds are generally cold. Tielens (2005) summarizes calculated cooling rates for interstellar molecular clouds. According to Tielens (2005), Cooling rates basically depends upon the abundances or, more precisely, on the ratio of the abundance to the velocity gradient, which sets the optical depth of the transitions involved. At low densities, CO dominates the cooling because of its high abundance in molecular clouds. Around a density of 10^3 cm^{-3} contribute to the cooling. Following Tielens (2005), we have included the cooling rate as a function of the H_2 number density of the cloud.

According to (Tielens, 2005), the low energy cosmic rays (CR) (~1–10 MeV) are the most efficient for ionizing and heating the gas. Here also, we consider only the effects of the cosmic rays for the process of gas heating. According to (Tielens, 2005), Cosmic ray heating rate can be represented as the following:

$$R_{CR} = n\zeta_{CR} E_h(E, xe), \quad (13)$$

where, ζ_{CR} is the total cosmic ray ionization rate (3×10^{-16} s^{-1} by assuming primary ionization rate 2×10^{-16} s^{-1}), n is the number density in the units of cm^{-3} and $E_h(E, x_e)$ is the average heat deposited per primary ionization. For the low degree of ionization, $E_h(E, x_e) \sim 7$ eV. In this case, the above equation becomes,

$$R_{CR} = 3 \times 10^{-27} n \frac{\zeta_{CR}}{2 \times 10^{-16}} \ erg \ \text{cm}^{-3} \ \text{s}^{-1}. \quad (14)$$

During various chemical reactions, heats are released/absorbed. But we have noticed that these rates are comparatively much lower than the other heating and cooling terms discussed above. So in our simulation, we neglect effects of energy released or absorbed due to chemical reactions.

3. Results and discussion

We now present the results of the simulations for a concrete case. In Table 1, the parameters which are used to non-dimensionalize the TVD code are tabulated and in Table 2, the parameters which are used here are written in c.g.s. units. We consider an interstellar cloud having a size of 10^{17} cm (i.e., 0.03 parsec) and divide the entire cloud into the 64×64 logarithmically equal spaced grids along the x and z directions respectively. This may appear to be a low resolution run. However, we find little difference in the average thermodynamic properties of cloud between a 16×16 run and a 64×64 run. Since the main emphasis of this paper is to study the chemical evolution of a number of species which depends on the average properties of the cloud, any further refinement of the mesh may not be necessary at this stage.

The cloud is assumed to be axisymmetric. Initially (at time $t = 0$), we assume that the cloud contains some mass (having density 10^{-23} gm/cm^{-3} at each grid location). From the outer boundary, we start to inject matter at a constant rate with a density 10^{-17} gm cm^{-3}, inward radial velocity -2.5×10^3 cm/s (-ve sign indicates the inward flow) and angular rotation 10^{-14} s. In the TVD code, we use non-dimensional quantities with the density at the outer boundary as the unit of density and the length of the computational zone along the x-axis as the unit of length. A sink is kept at the center of the cloud and it is assumed that any matter going inside a particular radius (the threshold radius, R_c) contributes to the core mass. Time step to advance the global time is calculated by using Courant–Friedrichs–Lewy (hereafter, Courant) condition. To be on the safer side even smaller time steps are used (Courant factor 0.1).

Fig. 1 represents the time evolution of the density distribution of a collapsing cloud in the meridional plane. The density of the cloud increases with time as the matter is accreted. On the right side of the panel, a color box is shown to indicate the color codes of the number densities in the logarithmic scale. For instance, black corresponds to a very low density and yellow corresponds to a very high density (marked on the right). We note that with time, the grid is filled up with a high density matter. Meanwhile, with time, the matter content of the innermost grid at the center (indicated by a large black box) also increases.

The black sphere at the center does not mean the core. Our actual core is point-like at the center. However, we have assumed a sink radius (the black box) which is sucking the matter from the cloud and transferring it into the core. This is required for the purpose of our numerical scheme to realize the effect of the central object. It should be kept in mind that we were dealing with a logarithmic scale here. So the apparently large looking sink is really very mini scale in size (size of the sink is 4.06×10^{14} cm and the whole size of the cloud is 10^{17} cm).

To understand Fig. 1 more clearly, in Fig. 2, we show the time evolution of number densities at a plane which is situated at a height of $z = 4.53 \times 10^{14}$ cm. The reason behind choosing these particular height is that the innermost grid location at this height is just beyond R_c and thus we see the density distribution around the innermost grid of this plane as well. Along the x axis, we plot the distance along the x direction and along the z axis, we plot

Table 1
Units used in the TVD code.

Parameter	Value
Length	10^{17} cm
Velocity	3×10^{10} cm/s
Density	10^{-17} gm/cm^{-3}
Time	3.33×10^6 s

Table 2
Initial and boundary values in c.g.s. units.

Parameter	Value
Outer radius	10^{17} cm
Inner radius	10^{14} cm
Initial Density	10^{-23} gm/cm^3
Courant factor	0.1
Initial Core mass	0 gm
Velocity at outer x boundary	-2.5×10^3 cm/s
Angular rotation at outer x boundary	10^{-14} s^{-1}
Density at the outer x boundary	10^{-17} gm/cm^3
γ	5/3
Number of grids	64×64
Threshold radius	4.06×10^{14} cm

the density at each grid. The right panel indicates time at which the density distributions are plotted. To have an idea about how the mass of the core increases with time, in Fig. 3, the time evolution of the total amount of accreted matter through the threshold radius is shown. As the density around R_c increases, the accretion rate from the R_c also increases and as a result, the core mass increases rapidly.

In the present work, we assume that the gas is adiabatic. So the temperature is also changing dynamically. In Fig. 4, the temperature distribution throughout a plane (at a height of $z = 4.53 \times 10^{14}$ cm) of a cloud is shown at the end of the simulation (i.e., after 1×10^6 year). From Fig. 4, it is clear that the temperature increases as we enter deeper inside the cloud.

In order to perform a self-consistent study, we assume that the gas and the grains are coupled through the accretion process and the thermal evaporation processes. We assume that the species are physisorbed onto the dust grain (classical size grain $\sim 1000\,A^{\circ}$) having the grain number density $1.33 \times 10^{-12} \times n$, where n is the concentration of H nuclei in all forms. Following, Hasegawa et al. (1992),we assume that there are 156 surface reactions among the 118 neutral surface species in our grain chemistry network. Following Das and Chakrabarti (2011) and references therein, all the updated interaction energies are used in our grain surface network. In addition to a large grain chemistry network, a large network of gas phase chemistry following Woodall et al. (2007) is implemented. Following Majumdar et al. (2012), we add up some more gas phase reactions in our network to have an educated estimation about the biologically important interstellar species. Majumdar et al. (2012) performed a quantum chemical

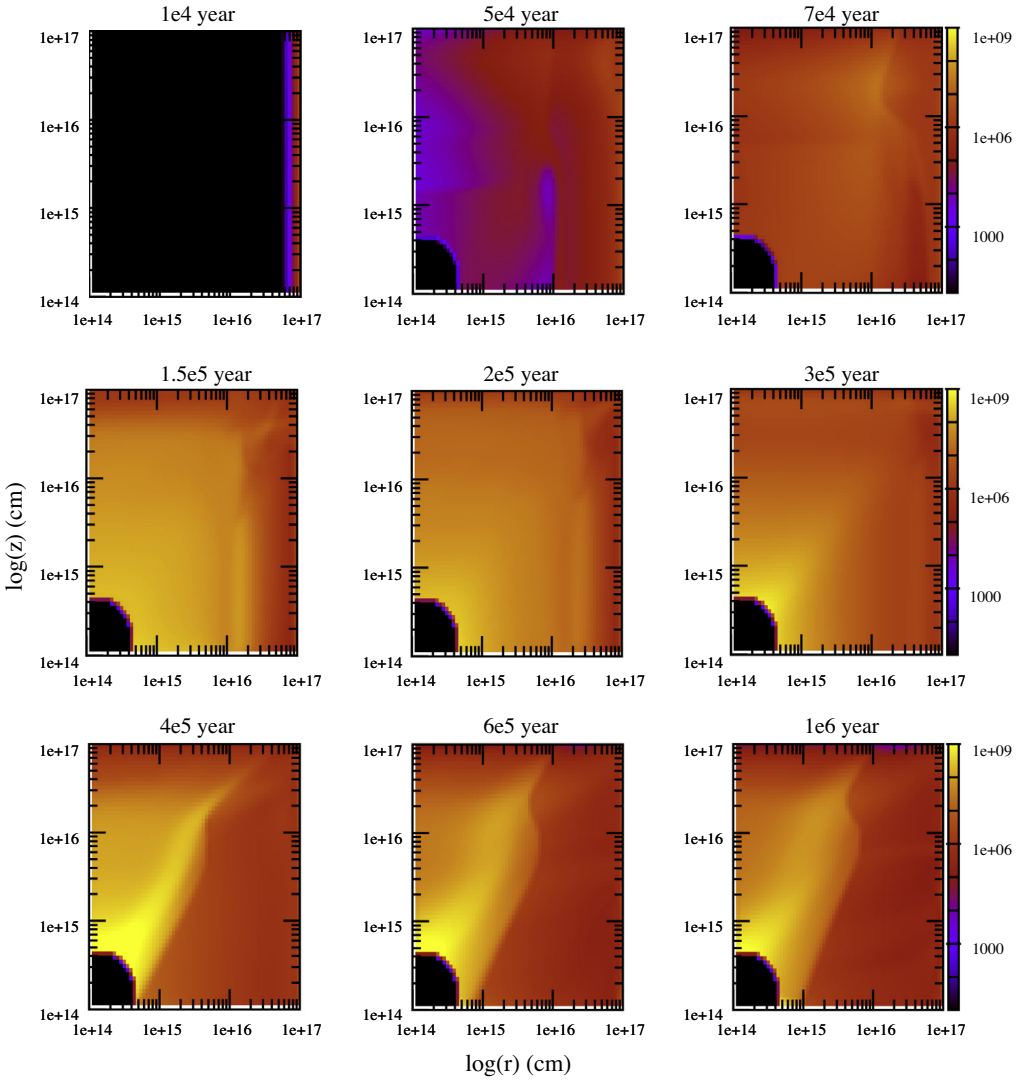

Fig. 1. Density distribution of a collapsing cloud in the meridional plane. Time is marked on each box. The color bar on the right can be used to get information about number density.

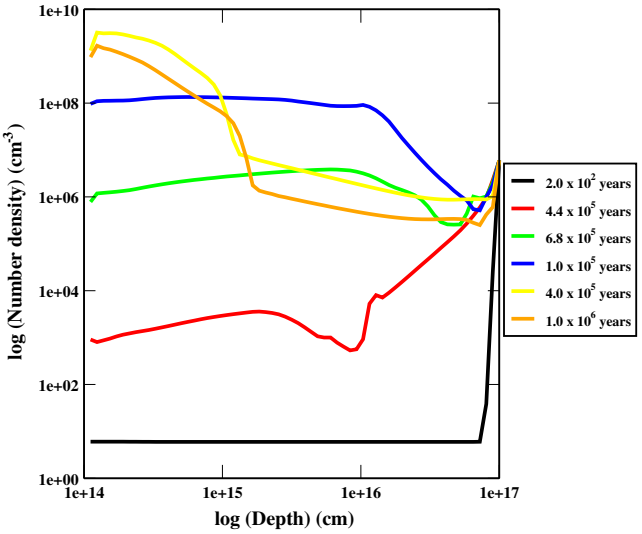

Fig. 2. Time evolution of the number densities for the plane at $z = 4.53 \times 10^{14}$ cm.

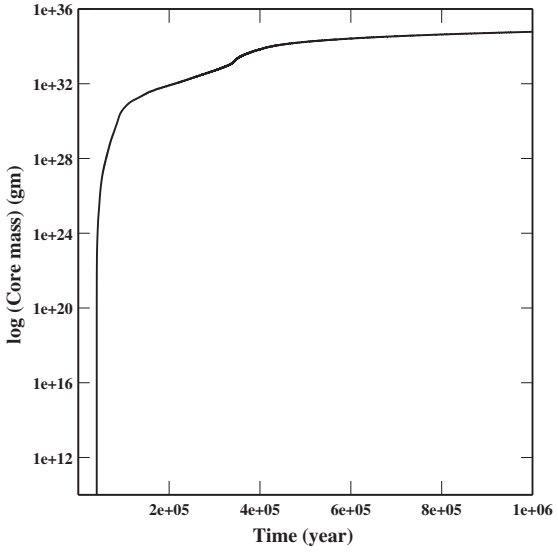

Fig. 3. Time evolution of the core mass is shown.

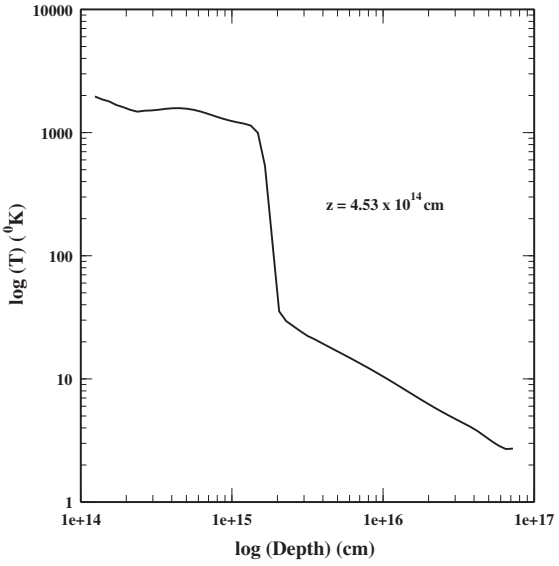

Fig. 4. Temperature distribution at $z = 4.53 \times 10^{14}$ cm plane.

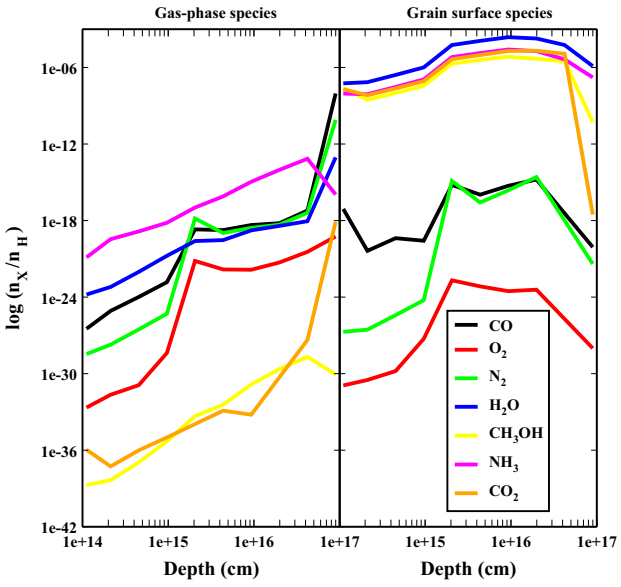

Fig. 5. Abundances of various major species in the gas and grain phases as the depth (x-coordinate) is varied at $z = 4.53 \times 10^{14}$ cm plane. Note that most of the region of cloud (gas phase/grain phase), H_2O dominates.

calculation to find out the reaction rates for the formation of some bio-molecules.

In our hydrodynamical model, we have 64×64 numerical grids. So in order to study the chemical evolution of the entire cloud, we need to study the chemical evolution at each numerical grids. In Fig. 5, we show the variation of the final abundances of some of the major interstellar gas-grain species for the plane at the height of 4.53×10^{14} cm). Here, we assume that the grain temperature remains constant at 10 K and vary gas temperature according to the outcome of the hydrodynamic code. Around the deep inside the cloud, density is much higher but it is also evident that the temperature is also much higher (Fig. 4). Abundances of several gas phase species are decreasing due to the heavy depletion to the grain surface. Since for the sake of simplicity, here we have assumed that grain temperature remain invariant at 10 K during the life time of the molecular cloud, most of the species locked into the grain surface due to the tight binding with the grain surface. Gas phase abundance around the deep inside the cloud also decreases due to the several favorable fragmentation reactions at the high temperatures. Stable species like H_2O, CH_3OH, CO_2, which are the major constituents of the grain mantle producing efficiently around the intermediate region of the collapsing cloud. Throughout the cloud, water is the most dominating molecule in the gas/grain phase.

3.1. Temperature dependent study

So far, we have carried out the simulations by keeping the grain temperature to be constant at $T = 10$ K. Gas phase temperature were taken from the hydrodynamic code. We have tested our case by assuming the actual temperature variations for the grains also. Consideration of the temperature effect, heavily affects the final results.

The molecular hydrogen is very abundant in the ISM. But this huge abundance cannot be explained unless we invoke the grain chemistry (Chakrabarti et al., 2006a,b). Gas phase H atoms land

on the dusty grains and produce molecular hydrogen via surface migration or Eley–Rideal method (direct accretion of one H on the top of another H atom) and finally they are evaporated from the grain surface and contribute to the gas phase abundances. For the better understanding, in Fig. 6, we have shown the depth dependence of the molecular hydrogen abundance at a height of $z = 4.53 \times 10^{14}$ cm. It is well known that around the 10–20 K, H_2 formation efficiency is maximum (Biham et al., 2001; Chakrabarti et al., 2006a,b). It is clear from Fig.6 that in case of the solid curve, H_2 is forming very efficiently around deep inside the cloud, whereas for the dotted curve it is producing around the intermediate region where temperature is much lower (10–20 K). This figure basically explains how the conversion of atomic hydrogen to the hydrogen molecule occurs at different depth of our simulated cloud. For the solid curve, we assume that grain temperature remain constant at 10 K and for the dotted curve, we consider more realistic case where the temperature variation of grains are also taken into account. In reality dotted curve is much more convenient to use since deep inside the cloud though the density is favorable for the formation of molecular hydrogen, temperature is much higher, as a result H2 production is not significant due to the short life time of the H atom on the grain surfaces.

In Fig. 7, we show the depth dependence of some of the major gas-grain species by considering the temperature dependency in the grain phase. For the better understanding of the difference between the two considerations (temperature dependency of grain and grain kept at 10 K), here also, we consider the same plane at $z = 4.53 \times 10^{14}$ cm as the earlier. Comparing Fig. 7 with the Fig. 5, we can clearly see that deep inside the cloud, the production over the interstellar grain is insignificant in Fig. 7. This is because, deep inside the cloud, the temperature is higher and all the molecules are likely to be evaporated from the grain surface and indeed the grain mantles themselves may evaporate, at least partly. Hence, around that region, the chemical enrichment of the interstellar medium is continued by the gas-phase chemistry alone. We have noticed that when we are considering the temperature variation, the effect of grain is found to be negligible inside of $\sim 2 \times 10^{15}$ cm. However, outside this radius, the temperature is cool enough for the production of several interstellar molecules on the grain surface. At the same time, as we go out from the

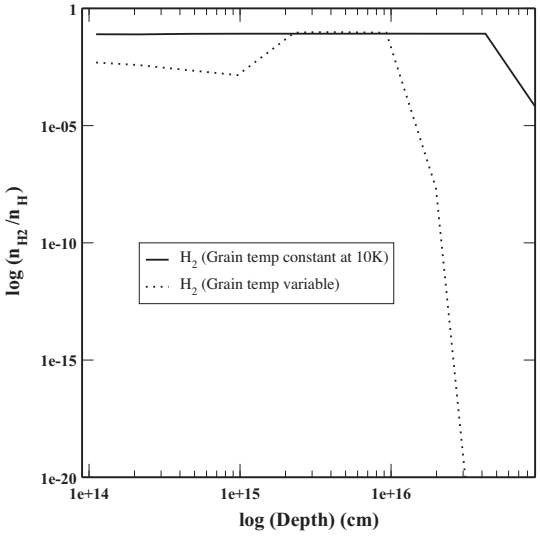

Fig. 6. Depth dependency of gas phase H_2 abundance is shown for different depth at $z = 4.53 \times 10^{14}$ cm plane. Solid curve is for the case where grain temperature is assumed to be constant at 10 K and dotted curve is for the case where grain temperature varies.

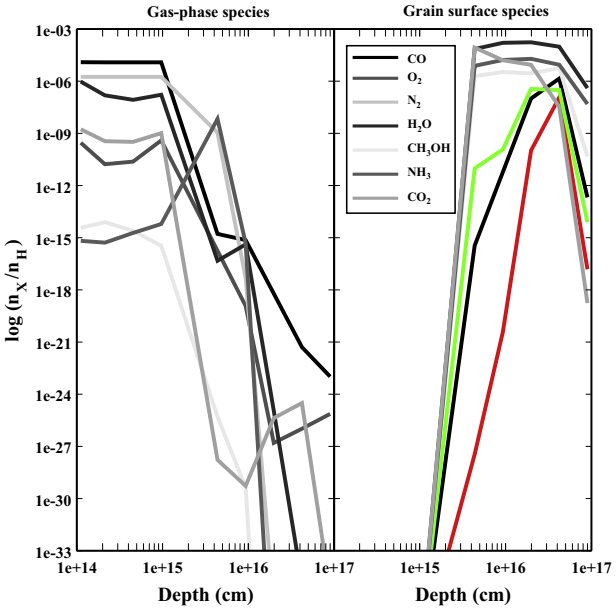

Fig. 7. Depth dependence of various simple species when the variation of grain temperature is also included.

central region, the density decreases, and the production on the grains significantly decreases. In case of the gas phase chemistry, deep inside the cloud, the temperature is higher but as the density is also higher, abundances are enhanced. In reality, the situation is very complex. Due to higher temperatures, the molecules dissociate easily into much smaller components. However, since the density is much higher also, they might be able to re-united again. So there is always a competition going on between the two effects: one due to density and other due to temperature.

For example, in case of Fig. 5, gas phase CO molecules are rapidly decreasing due to the heavy depletion on the grain surface, whereas in case of Fig. 7, due to the high temperature of the grain surface, CO molecules are unable to reside on the grain surface. As a result, their abundance in the gas phase increases. Production of surface species are noticed to be favorable around the low temperature region (8–30 K). From the temperature distribution (Fig. 4) of the cloud, it is evident that intermediate region of the cloud ($\sim 2 \times 10^{15} - 1.5 \times 10^{16}$ cm,) is also in the low temperature regime (8–30 K), so the production of surface related species are more favorable around the intermediate region of the cloud. From Fig. 7, it is also clear that production of the grain surface species decreases as we are going further out, especially because density is reduced with distance. At the much lower temperatures (<8 K), surface species also lost its mobility, as a results production also hindered in the grain phase also.

We believe that inside a molecular cloud bio-molecules might also be formed due to very complex and rich chemical process. Production of amino acids, nucleobases, carbohydrates and other basic compounds can possibly start from these bio-molecules. For the first time Chakrabarti and Chakrabarti (2000a,b) made an attempt to study the formation of bio-molecules (adenine, alanine, glycine, glycolic acid and lactic acid) during the collapsing phase of a protostar. They realized that major obstacle for studying the evolution of these interstellar bio-molecules are the lack of adequate knowledge of the rate co-efficients of various reactions which are taking place. In order to obtain more realistic abundances of interstellar bio-molecules, Majumdar et al. (2012) carried out quantum chemical simulation to find out the reaction rate coefficients for the formation of these interstellar bio-molecules. Here, we have included the chemical network for the formation of these bio-molecules by

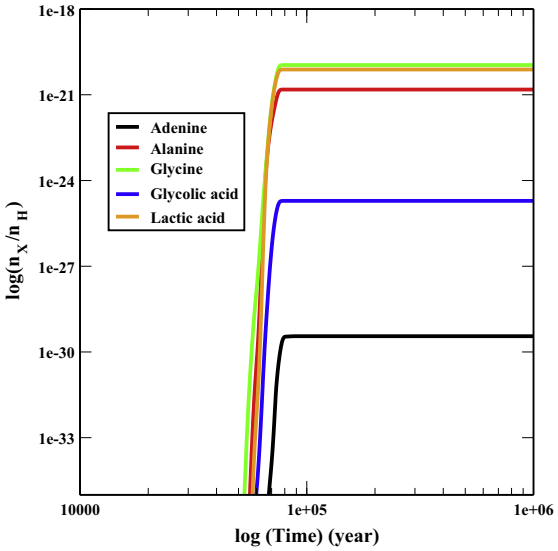

Fig. 8. Time evolution of some of the pre-biotic molecules.

following Chakrabarti and Chakrabarti (2000a,b), Majumdar et al. (2012).

In Fig. 8, we have shown the chemical evolution of some important bio-molecules at a grid location $X = 9.3 \times 10^{15}$ cm, $Z = 4.53 \times 10^{14}$ cm, where temperature is around 10 K, which is favorable for the production of complex molecules. Computed abundances of these molecules are $1.1 \times 10^{-20}, 1.53 \times 10^{-21}, 3.57 \times 10^{-30}, 7.66 \times 10^{-21}, 1.94 \times 10^{-25}$ for glycine, alanine, adenine, lactic acid & glycolic acid respectively. Majumdar et al. (2013) made a rigorous attempt to identify the precursor of adenine, alanine & glycine which could be observed in the ISM. According to them NH_2CN and HCCN are the precursors of adenine, C_2H_3ON is the precursor of glycine and C_3H_5ON is the precursor of alanine. They also reported their respective infrared and electronic absorption spectra. Here, our computed abundances are well below the observational limit, thus as Majumdar et al. (2013), we are also proposing to predict the abundances of these molecules by observing its pre-cursor molecules. Spectral information of these pre-cursor molecules are already discussed in detail in Majumdar et al. (2013). To set a observational guidelines for predicting the abundance of these bio-molecules, as like Das et al. (2013), we are now trying to report the rotational spectral information of these pre-cursor molecules elsewhere soon in the format of JPL/CDMS catalog.

3.2. Comparison with previous models

Main emphasis of the present paper is upon the chemical evolution of a more realistic cloud by considering a two dimensional hydrodynamical flow which includes rotation and heating & cooling of the ISM whereas our earlier paper (Das et al., 2008a) mainly focuses on the chemical evolution of a spherically symmetric isothermal collapsing cloud. Our present chemical model is more up to dated as here we have used UMIST 2006 database (Woodall et al., 2007) for our gas phase chemical network and have included recently computed rate coefficients for the formation of several bio-molecules (Majumdar et al., 2012). In our earlier model, we considered grain chemistry only for the formation of molecular hydrogen, here we are using a large surface chemical network (Hasegawa et al., 1992; Das et al., 2010; Das and Chakrabarti, 2011) to self-consistently study the chemical evolution of a collapsing cloud. In our earlier paper as we have considered an isothermal cloud, chemical evolution was mainly dependent upon the density of any region, whereas, in the present model, temperature is also an important parameter for deciding the degree of chemical enrichment. To avoid complexity in this paper, we have studied the chemical evolution at a particular height ($Z = 4.53 \times 10^{14}$ cm), but in principal we could have studied it for the whole cloud. This is out of scope of this paper and we are now in preparation to report it elsewhere. Since the chemical evolution heavily dependent upon the physical parameters (density & temperature), abundances of all the species would expected to be different along different region.

Hasegawa et al. (1992) prepared a gas-grain model and studied the time evolution of the chemical species for a steady state cloud ($n = 2 \times 10^4$ cm^{-3}, T = 10 K and A_V=500). Stantcheva and Herbst (2004) prepared models of gas-grain chemistry in interstellar cloud cores ($n = 2 \times 10^4$ cm^{-3}, T = 10 – 20 K) with a stochastic approach to surface chemistry. For both the cases it was observed that as time is evolving, CO molecules are heavily depleted from the gas phase and the abundance of CO and its related surface species (CO_2, H_2CO, CH_3OH) gradually increases over the time being. Our model mainly differs due to the physical properties of the cloud considered here. In this paper, we are adopting the physical properties from the outcome of our updated hydrodynamical model, whereas they considered a static cloud condition. Here, Fig.7, shows that deep inside the cloud, abundances of gas phase CO molecules are much higher whereas in Das et al. (2008a) it was shown that deep inside the cloud gas phase CO molecules are depleted to the grain surface. In Das et al. (2008a), it was assumed that cloud remain in isothermal stage during the collapsing phase. So, as we are going deep inside the cloud, since the density is increasing, probability of freezing to the grain surface increases simultaneously. But in reality, as we are going inside a collapsing cloud, its temperature increases gradually (Fig. 4), and the probability of freezing gradually diminishes. Since in Fig. 7, effect of temperatures are included, it is showing apparently the real depth dependency of a collapsing cloud.

In Das et al. (2008a), abundances of alanine & glycine were computed by assuming an average reaction rate coefficients $\sim 10^{-10}$ cm^{3}s^{-1}. Computed abundances of alanine and glycine from Das et al. (2008a) was $2.3 - 8.3 \times 10^{-17}$ and $1.7 - 2.9 \times 10^{-14}$ respectively. With the modified rate coefficients, Majumdar et al. (2013) predicted the peak abundance of alanine and glycine to be 8.9×10^{-18} and 1.96×10^{-17} respectively. Our computed abundances of the alanine and glycine are 1.53×10^{-21} and 1.1×10^{-20} respectively. Chakrabarti and Chakrabarti (2000a) predicted the abundances of adenine to be 6.35×10^{-11} whereas Majumdar et al. (2012, 2013) predicted adenine abundance to be 4.4×10^{-25}. In our present context adenine abundance found to be 3.57×10^{-30}. Main difference for the production of bio-molecules between Das et al. (2008a); Chakrabarti and Chakrabarti (2000a,b), Majumdar et al. (2012, 2013) along with the present paper is the usage of rate coefficients during the formation of these molecules. To have an educated estimation for the production of bio-molecules (alanine, glycine & adenine), in Das et al. (2008a) and Chakrabarti and Chakrabarti (2000a,b), rate coefficients were assumed to be $\sim 10^{-10}$ cm^{3}s^{-1} whereas in Majumdar et al. (2013) and present paper, rate coefficients were taken from Majumdar et al. (2012). Moreover, Since Das et al. (2008a) and Chakrabarti and Chakrabarti (2000a,b) did not consider the extensive surface chemistry network, their computed gas phase abundances does not seems to be depleted whereas due to the consideration of a large surface chemistry network, related chemical species of selected bio-molecules could be depleted on the grain surface which could affect their gas phase abundances. Differences between the results of Majumdar et al. (2012, 2013) & the present paper are unsurprising because here, we are using totally different physical

conditions (elaborately mentioned in the earlier sections) in comparison to the Majumdar et al. (2012, 2013).

4. Conclusions

In this paper, we carry out numerical simulations to find out the abundances of different interstellar molecules inside a collapsing and rotating interstellar cloud. A well tested two dimensional hydrodynamics code has been used to obtain the physical properties during the collapsing phase of a generic molecular cloud. Mechanisms which are responsible for the interstellar heating and cooling are considered. The dynamic behavior of the interstellar cloud during the collapsing phase are used as the input parameter for the chemical code. Major improvements over the chemical model considered in Das et al. (2008a) are the inclusion of the grain chemistry self-consistently and the inclusion of gas phase chemical network from the UMIST 2006 data base (Woodall et al., 2007; Chakrabarti and Chakrabarti, 2000a,b; Majumdar et al., 2012). A detail comparison between our present work with our earlier work along with some other important modeling results are highlighted.

Temperature is an important physical parameters for a deciding the molecular complexity of a molecular cloud. We carried out our simulation with both the constant temperature and varying the temperature of the cloud. Results clearly shows strong variation in between these two consideration.

So far we have chosen only a single rotation parameter just to show its effect. With the increase of rotational velocity, the centrifugal force would remove a large amount of matter in the outer regions, especially along the axis of the cloud. These bi-polar flows would have significant effects as they would carry away chemicals produced deep inside and distribute them at outer regions. Part of this chemically enriched matter could be farther reprocessed as it is accreted again along with inflow. Furthermore, a stronger centrifugal force would create shock waves changing the density and temperature distribution dramatically which in turn would also modify chemical abundances. This aspect is being studied throughly and would be reported elsewhere.

Acknowledgments

SKC, LM & SC are grateful to DST for the financial support through a project (Grant No. SR/S2/HEP-40/2008) and AD wants to thank ISRO respond project (Grant No. ISRO/RES/2/372/11-12). We would like to acknowledge D. Ryu from Chungnam National University, Daejeon, Korea for his suggestions in developing the TVD code with self-gravity.

References

Allen, M., Robinson, G.W., 1977. APJ 212, 396.
Biham, O., Furman, I., Pirronello, V., Vidali, G., 2001. APJ 553, 595.
Chakrabarti, S.K., Chakrabarti, S., 2000a. Indian J. Phys. Part B 74B (2), 97.
Chakrabarti, S., Chakrabarti, S.K., 2000b. A&A 354L, 6.
Chakrabarti, S.K., Das, A., Acharyya, K., Chakrabarti, S.K., 2006a. A&A 457, 167.
Chakrabarti, S.K., Das, A., Acharyya, K., Chakrabarti, S.K., 2006b. BASI 34, 299.
Das, A., Chakrabarti, S.K., 2011. MNRAS 418, 545.
Das, A., Chakrabarti, S.K., Acharyya, K., Chakrabarti, S., 2008a. NEWA 13, 457.
Das, A., Acharyya, K., Chakrabarti, S., Chakrabarti, S.K., 2008b. A & A 486, 209.
Das, A., Acharyya, K., Chakrabarti, S.K., 2010. MNRAS 409, 789.
Das, A., Majumdar L., Chakrabarti S.K., Saha, R., Chakrabarti, S., 2013, MNRAS (communicated).
Harten, A., 1983. J. Comp. Phys. 49, 357.
Hasegawa, T., Herbst, E., Leung, C.M., 1992. APJ 82, 167.
Majumdar, L., Das, A., Chakrabarti, S.K., Chakrabarti, S., 2012. RAA 12, 1613.
Majumdar, L., Das, A., Chakrabarti, S.K., Chakrabarti, S., 2013. New Astronomy 20, 15.
Roe, P.L., 1981. J. Comp. Phys. 43, 357.
Ryu, D., Ostriker, J.P., Kang, H., Cen, R., 1993. APJ 414, 1.
Stantcheva, T., Herbst, E., 2004. A&A 423, 241.
Tielens, A.G.G.M., 2005. The Physics and Chemistry of Interstellar Medium. Cambridge Univ. Press, Cambridge.
Van Dishoeck, E.F., Blake, G.A., 1998. ARAA 36, 317.
Woodall, J., Agndez, M., Markwick-Kemper, A.J., Millar, T.J., 2007. A&A 466, 1197.